This article is published as part of the *Dalton Transactions* themed issue entitled:

New Talent

Showcasing the strength of research being carried out by tomorrow's leaders in the field of inorganic chemistry

Guest Editor Polly Arnold
University of Edinburgh, UK

Published in issue 2, 2010 of *Dalton Transactions*

Image reproduced with permission of Mark Muldoon

Articles in the issue include:

PERSPECTIVES:

Modern multiphase catalysis: new developments in the separation of homogeneous catalysts
Mark J. Muldoon, *Dalton Trans.,* 2010, DOI**:** 10.1039/b916861n

Probing bioinorganic chemistry processes in the bloodstream to gain new insights into the origin of human diseases
Elham Zeini Jahromi and Jürgen Gailer, *Dalton Trans.,* 2010, DOI: 10.1039/b912941n

COMMUNICATIONS:

Facile entry to 3d late transition metal boryl complexes
Ba L. Tran, Debashis Adhikari, Hongjun Fan, Maren Pink and Daniel J. Mindiola**,**
Dalton Trans., 2010, DOI: 10.1039/b912040h

Probing the kinetics of ligand exchange on colloidal gold nanoparticles by surface-enhanced raman scattering
Yuhua Feng, Shuangxi Xing, Jun Xu, Hong Wang, Jun Wei Lim and Hongyu Chen,
Dalton Trans., 2010, DOI: 10.1039/b912317b

Visit the *Dalton Transactions* website for more cutting-edge inorganic and organometallic research
www.rsc.org/dalton

Bis(oxazolinyl)phenylborane: A Lewis acid-containing ligand for methide abstraction-based coordination to aluminum(III)†

James F. Dunne, Kuntal Manna, Jerzy W. Wiench, Arkady Ellern, Marek Pruski and Aaron D. Sadow*

Received 17th June 2009, Accepted 21st September 2009
First published as an Advance Article on the web 27th October 2009
DOI: 10.1039/b911851a

A compound that contains a Lewis acidic boron center and coordinating oxazoline groups, bis(4,4-dimethyl-2-oxazolinyl)phenylborane (**PhB(Ox^{Me2})$_2$**; **1**), has been prepared and spectroscopically characterized. Solvent dependent ^{15}N and ^{11}B NMR spectroscopic properties and solid-state ^{11}B NMR measurements provide support for intermolecular interactions involving Lewis acid and base sites. The bifunctional nature of oxazolinylborane **1** is demonstrated by its reaction with $(AlMe_3)_2$, which proceeds *via* methide abstraction by the boron and oxazoline coordination to aluminum to yield [(κ^2-PhMeB(Ox^{Me2})$_2$AlMe$_2$] (**2**). Compound **2** contains a planar six-membered chelate ring, in contrast to related bis(pyrazolyl)boratoaluminum compounds that are puckered. Additionally, compound **2** and related bidentate tris(oxazolinyl)phenylborato dimethylaluminum are inert toward aluminum-methyl bond protonolysis. This robust nature suggested the possibility of using these oxazolinylborato-aluminum compounds in catalytic reactions, as is demonstrated by lactide ring-opening polymerization.

Introduction

The salt metathesis reaction is a powerful method for the introduction of one or more anionic ligands in inorganic synthesis. In some instances however, alternative synthetic routes are desired because problems in salt metathesis steps can occur, including electron transfer reactions, incomplete salt elimination, and poor control over stoichiometry. For example, the protonolytic elimination reaction is particularly effective for the introduction of anionic ancillary ligands to d^0 metal complexes (eq. 1). In these transformations, a Brønsted acidic proligand H[LX] and a basic anionic group bonded to a metal center [MR$_n$] react to (formally) open a coordination site for the incoming ligand to bind. Another method, pioneered by Parkin, combines a ligand salt and a metal alkyl complex to form the desired ligand-metal structure with concurrent elimination of RM′ (eq. 2).[1] Still, new methods for the introduction of anionic ligands to metal centers could be valuable in synthetic chemistry.

$$MR_n + H(LX) \longrightarrow (LX)MR_{n-1} + R\text{–}H \quad (1)$$

$$MR_n + M'(LX) \longrightarrow (LX)MR_{n-1} + R\text{–}M' \quad (2)$$

The metathesis and protonolysis-based methods described above formally involve abstraction of an anionic ligand from a metal complex. A synthetic method that applies this general concept might involve a proligand that contains a Lewis acid site to act as an abstraction agent rather than a Brønsted acid that mediates a protonolytic elimination. The reaction of an organometallic precursor and a Lewis acid-containing proligand would provide a direct route to zwitterionic metal complexes.[2] In this context, phosphino-borane,[3] phosphino-alane,[4] and phosphino-gallane[5] ambiphilic ligands react with transition metal complexes by coordination of the phosphine and abstraction of an anionic alkyl or halide ligand. In some cases, more reactive metal complexes are obtained. For example, Fontaine and Zargarian showed that $Me_2AlCH_2PMe_2$ provides a more reactive nickel(II) catalyst for phenylsilane polymerization than a simple phosphine.[4a]

Tris(perfluorophenyl)borane provides an ideal Lewis acid site, since it is effective for hydrocarbyl abstraction to give either zwitterionic or charge-separated ionic complexes.[6] Thus, our proligand design contains a boron center as the Lewis acid. Additionally, 2-oxazolines are appealing as coordinating groups because the imidine nitrogen is a relatively weak donor and the oxazoline α-carbon (that is bonded to boron) is inductively electron-withdrawing which could enhance the boron's Lewis acidity. The resulting borane can participate in abstraction chemistry upon interaction with organometallic compounds providing unsymmetrical phenyl(alkyl)bis(oxazolinyl)borato complexes (as shown in eq. 3).

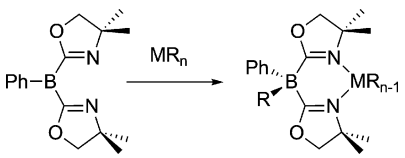

(3)

These oxazolinylborates are a promising new ligand class, as demonstrated by Pfaltz in stereoselective catalytic transformations.[7] Thus, C_2-symmetric bis(2-oxazolinyl)borates were recently prepared, introduced to copper, iridium, and palladium through salt metathesis, and used effectively in stereoselective cyclopropanation and allylic alkylation reactions.[7] A number of boron containing cyclopentadienyl compounds have been prepared and their transition metal chemistry has been investigated.[8] However, concurrent metal alkyl abstraction/metal coordination reactions have not been described with those ligands.

Department of Chemistry and US Department of Energy Ames Laboratory, Iowa State University, 1605 Gilman Hall, Ames, Iowa 50011-3111, USA

† Electronic supplementary information (ESI) available: Additional experimental details. CCDC reference number 736433. For ESI and crystallographic data in CIF or other electronic format see DOI: 10.1039/b911851a

Here we report the preparation of bis(4,4-dimethyl-2-oxazolinyl)phenylborane (**PhB(Ox^{Me2})$_2$**; **1**), the first neutral oxazolinylborane compound. Its solution structure has been inferred from solvent dependent ^{15}N and variable temperature ^{11}B NMR spectroscopic data, which revealed the presence of both Lewis acid and Lewis base sites in **1**. Solid-state 2D ^{11}B and ^{1}H NMR experiments further substantiated the structural assignments and provided evidence for intermolecular aggregation. Reaction of compound **1** with trimethylaluminum affords a zwitterionic bis(oxazolinyl)borato aluminum organometallic complex [(κ^2-PhMeB(Ox^{Me2})$_2$)AlMe$_2$] (**2**). The structure of **2** is compared to the isoelectronic planar {BOX-Me$_2$}AlCl$_2$[9] and puckered poly(pyrazolyl)boratoaluminum compounds.[10-13] The Al-Me bonds in compound **2** are surprisingly inert toward protonation, especially in comparison to pyrazolylborate aluminum compounds. Due to this robust nature, the reactivities of **2** and related tris(oxazolinyl)boratoaluminum compounds were investigated in lactide ring-opening polymerization.

Results and discussion

Synthesis and characterization of PhB(Ox^{Me2})$_2$ (1)

Reaction of 4,4-dimethyl-2-oxazoline (**2H-Ox^{Me2}**) and *n*-BuLi (THF, –78 °C) gives 2-lithio-4,4-dimethyl-2-oxazolide (**2Li-Ox^{Me2}**) as first described by Meyers and Collington.[14] Addition of 0.5 equiv. of PhBCl$_2$ to this oxazolide provides the desired bis(4,4-dimethyl-2-oxazolinyl)phenylborane (**PhB(Ox^{Me2})$_2$**; **1**) after 14 h (eq. 4).

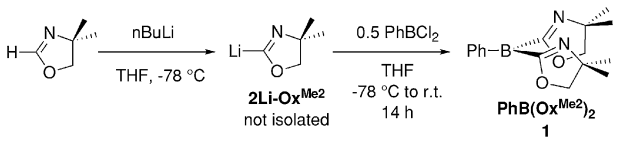

(4)

Pfaltz and co-workers previously reported the preparation of bis(2-oxazolinyl)diphenylborates by reaction of oxazolide anions and 0.5 equiv. of Ph$_2$BCl,[7] and Lambert *et. al.* described the synthesis of (benzoxazolyl)triphenylborate from benzoxazolide and Ph$_3$B.[15] However, **1** is apparently the first oxazolinyl-containing neutral borane. Another borane that contains donor groups, PhB(CH$_2$P^{t}Bu$_2$)$_2$, was recently prepared as an intermediate that, upon treatment with lithium pyrazolate, affords mixed bis(phosphino)-pyrazolyl borate compounds Li[PhB(CH$_2$P^{t}Bu$_2$)$_2$(N$_2$C$_3$R$_2$H)] (R = H, Me).[16] However, poly(pyrazolyl)boranes that might be comparable to PhB(Ox^{Me2})$_2$ have not been described; since poly(pyrazolyl)borates are typically prepared through pyrazole-borohydride condensation reactions, the corresponding boranes are not accessible. Unfortunately, the chiral derivative from the enantiopure *4S*-isopropyl-2-oxazoline could not be isolated under our synthetic conditions; reactions of 2 equiv. of isolated 2-lithio-*4S*-isopropyl-2-oxazolide and PhBCl$_2$ provide inseparable mixtures of bis(*4S*-isopropyl-2-oxazolinyl)borane and lithium tris(*4S*-isopropyl-2-oxazolinyl)borate (**Li[To^P]**), identified by ^{11}B NMR spectroscopy and comparison to authentic samples of Li[To^P].[17]

The ^{1}H, ^{15}N, and ^{11}B NMR spectroscopic properties of borane **1** are solvent and temperature dependent, and the relevant values are listed in Table 1. These data, described below, are consistent with intermolecular oxazoline-boron interactions. The ^{1}H NMR spectrum of **1** was broad in toluene-d_8 at room temperature, elevated temperature (to 353 K), and low temperature (to 200 K). A well-resolved spectrum was obtained in acetonitrile-d_3 (room temperature) that contained two diastereotopic methyl resonances and two coupled doublets at 3.64 and 3.57 ppm ($^2J_{HH}$ = 8 Hz) corresponding to diastereotopic methylene groups. A similar well-resolved pattern was observed for the room temperature ^{1}H NMR spectrum of **1** in methanol-d_4, and in both cases the diastereotopic oxazoline signals indicated that the compound's symmetry is C_s or C_2 (but not C_{2v} or higher). A single ^{15}N{^{1}H} NMR resonance for **1** (–147.0 ppm in acetonitrile-d_3, observed through a ^{1}H-^{15}N HMBC experiment) is consistent with two symmetry-related oxazoline rings. This value is shifted upfield by 18 ppm from that of 2H-Ox^{Me2} (–128.9 ppm, acetonitrile-d_3), which suggests that the oxazoline nitrogen in **1** are interacting with an electrophilic center (*i.e.*, a boron in another molecule of **1**). The ^{15}N NMR chemical shifts of these oxazoline species have significant solvent dependence (see Table 1): in methanol-d_4, the values for 2H-Ox^{Me2} (–139.4 ppm) and **1** (–169.9 ppm) are shifted by 10.5 and 22.9 ppm upfield, respectively, from those measured in acetonitrile-d_3. Additionally, the chemical shift difference between 2H-Ox^{Me2} and **1** is significantly larger in methanol-d_4 (30.5 ppm) than in acetonitrile. We suspected that the solvent dependent ^{1}H NMR spectral resolution and ^{15}N NMR chemical shifts of **1** were related to methanol-d_4 or acetonitrile-d_3 coordination to the boron center and the presence of alcohol functionality in methanol-d_4. Unfortunately, ^{15}N NMR data could not be obtained in non-coordinating solvents such as benzene-d_6 because the ^{1}H NMR spectrum was broad. Thus ^{11}B NMR spectra were collected to probe this possibility.

Table 1 ^{15}N and ^{11}B NMR chemical shift values for oxazoline, oxazolinylborane, and oxazolinylborate compounds

Compound	Solvent	^{15}N NMR (δ)	^{11}B NMR (δ)
2H-Ox^{Me2}	benzene-d_6	–127.5	no boron present
2H-Ox^{Me2}	tetrahydrofuran-d_8	–127.9	no boron present
2H-Ox^{Me2}	acetonitrile-d_3	–128.9	no boron present
2H-Ox^{Me2}	methanol-d_4	–139.4	no boron present
PhB(Ox^{Me2})$_2$ (**1**)	toluene-d_8, 220 K	not available	–5.2 and –11.0
1	acetonitrile-d_3	–147.0	–8.1
1	methanol-d_4	–169.9	–4.1
PhMeB(Ox^{Me2})$_2$AlMe$_2$ (**2**)	benzene-d_6	–186.7	–16.7
(κ^2-To^M)AlMe$_2$ (**3**)	benzene-d_6	–120.2 (pendent), –184.2 (coordinated)	–16.5
[(PhB(Ox^{Me2}H)(Ox^{Me2})$_2$)AlMe$_2$] (**4**)	benzene-d_6	–202.2 (protonated), –176.9 (coordinated)	–12.4

The ^{11}B NMR spectrum of **1** in acetonitrile-d_3 contained one broad singlet at −8.1 ppm (width at half-height, $\Delta\nu_{1/2}$ = 138 Hz). Comparison with ^{11}B NMR chemical shifts and linewidths of the lithium salt of tris(4,4-dimethyl-2-oxazolinyl)phenylborate (**Li[To^{M}]**, −17.0 ppm in acetonitrile, $\Delta\nu_{1/2}$ = 12.5 Hz)[18] and lithium bis(4S-^{i}Pr-2-oxazolinyl)diphenylborate (−12.7 ppm)[7] suggests that **1** contains a neutral boron center. However, the upfield chemical shift is more consistent with a neutral four-coordinate boron center than a three-coordinate center and suggests that a neutral donor (*i.e.*, acetonitrile-d_3) is coordinated to boron.[19] In methanol-d_4, the ^{11}B NMR spectrum also contained a single broad resonance (−4.1 ppm, $\Delta\nu_{1/2}$ = 82 Hz) that was slightly downfield from that observed in acetonitrile-d_3. These observations suggest that solvent coordination to the Lewis acidic boron center gives the adducts PhB(Ox^{Me2})$_2$·NCMe or PhB(Ox^{Me2})$_2$·HOMe that have different ^{11}B NMR chemical shift values. For comparison, $BH_3(OEt_2)$ and $BH_3(NMe_3)$ ^{11}B NMR chemical shifts (2.5 and −8.1 ppm, respectively) follow the same trend.[19b]

In non-coordinating toluene-d_8 solvent, **1** does not provide an observable signal in ^{11}B NMR spectra acquired at room temperature or at elevated temperature (350 K). However, two ^{11}B NMR resonances were detected at −5.2 and −11.0 ppm in a spectrum acquired at 220 K. Comparison of these low temperature chemical shift values to those obtained for methanol and acetonitrile adducts of **1** suggest that intermolecular *O*-oxazoline and *N*-oxazoline coordination provides two distinct boron sites. At room temperature in non-coordinating solvent (toluene-d_8 or benzene-d_6), the exchange process is in the intermediate regime, which obscures the signals.

The intermolecular B-O and B-N interactions were further investigated by solid-state ^{11}B NMR spectroscopy. Multidimensional solid-state NMR can provide detailed information about species' local environment based on peak shape and/or position, and identify intermolecular interactions *via* through-space ^{1}H-^{11}B magnetization transfer. The solid-state ^{11}B NMR spectrum of PhB(Ox^{Me2})$_2$ (**1**), acquired under magic angle spinning (MAS) at 20 kHz (Fig. 1a), contained multiple resonances from +7 to −15 ppm assigned to four-coordinate boron centers, and a broad resonance centered at 22 ppm assigned to a tricoordinated boron species in PhB(Ox^{Me2})$_2$ that is not observed in solution. Further interpretation of this ^{11}B MAS spectrum is difficult because the central transitions of nonsymmetrically substituted boron sites are affected by the anisotropic quadrupolar interaction, which manifests itself in the presence of broad and complex

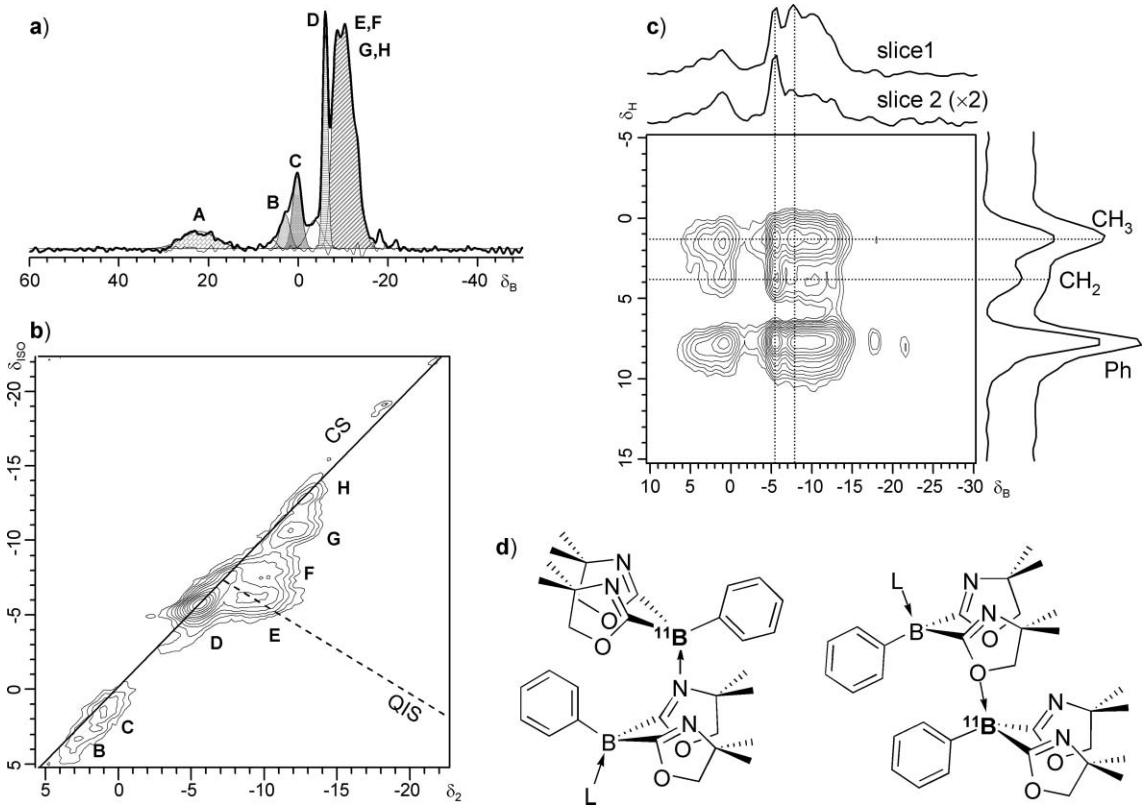

Fig. 1 (a) ^{11}B MAS, (b) ^{11}B MQMAS, and (c) ^{1}H-^{11}B HETCOR spectra of PhB(Ox^{Me2})$_2$ in the solid state. (d) Proposed intermolecular *N*- and *O*-oxazoline boron interactions. Spectrum (a) was deconvoluted using the lineshape parameters for species B through H determined from spectrum (b). In spectrum (b) the chemical shift (CS) and quadrupolar-induced shift (QIS) axes are shown using solid and dashed lines, respectively.[23] Spectrum (c) was acquired using homonuclear PMLG-5 ^{1}H decoupling during ^{1}H evolution in t_1.[24] Dotted lines in (c) indicate positions of selected cross-sections displayed along the vertical (^{1}H) and horizontal (^{11}B) axes. The experimental conditions were as follows: B_0 = 14.1 T, ν_R = 20 kHz; for spectrum (a): ν^B_{RF} = 83 kHz, the nutation angle = 15°, τ_{RD} = 12.5 s; for spectrum (b): ν^B_{RF} during hard pulses = 83 kHz, ν^B_{RF} during soft (z-filter) pulse = 14.7 kHz, τ_{RD} = 3 s, States method was used with 120 t_1 increments of 50 μs, NS = 48, AT = 9.5 h; for spectrum (c): τ_{CP} = 500 μs, ν^H_{RF} during cross polarization (CP) = 22 kHz (tangently ramped ±1 kHz), ν^B_{RF} during CP = 2 kHz, ν^H_{RF} during PMLG-5 decoupling = 135 kHz, States-TPPI method was used with 166 t_1 increments of 60 μs, τ_{RD} = 1.2 s, NS = 80, and AT = 9 h.

Table 2 Shifts and quadrupolar parameters determined from ^{11}B MQMAS spectrum

Site	δ_2[a]	δ_{ISO}[a]	δ_{QIS}[a]	δ_{CS}[a]	P_Q[b]	mol%
A	22	—	—	—	—	8
B	2.5	3.2	0.4	2.9	0.8	5
C	0.8	1.4	0.4	1.2	0.7	9
D	−5.8	−5.8	0.0	−5.8	0.0	15
E	−9.5	−6.1	2.1	−7.4	1.8	
F	−10.3	−7.8	1.6	−8.7	1.5	
G	−12.2	−10.7	0.9	−11.3	1.2	63[c]
H	−13.0	−12.8	0.1	−12.9	0.4	

[a] δ_2—the NMR shift observed in single-quantum (MAS) dimension, δ_{ISO}—the isotropic shift observed in multiple-quantum dimension, δ_{QIS}—the quadrupolar-induced shift, δ_{CS}—the chemical shift. All shifts are given in ppm from $BF_3{\cdot}Et_2O$. [b] Second order quadrupolar effect, defined as $P_Q = C_Q\sqrt{1+\eta_Q^2/3}$, where C_Q is the quadrupole coupling constant and η_Q is the asymmetry parameter (in MHz). [c] species E, F, G and H combined.

powder patterns.[20] Due to the presence of multiple species, the ^{11}B MAS spectrum consists of strongly overlapping features, making the deconvolution very unreliable. In addition, the quadrupolar interaction shifts the resonances away from the chemical shift positions observed in solution. When multiple species are present, the deconvolution of such a spectrum cannot be reliably performed without additional information. Therefore, a 2D MQMAS (multiple quantum magic angle spinning) experiment was carried out (Fig. 1b),[21] which suppresses the quadrupolar broadening and allows the separation of isotropic chemical shifts (δ_{CS}) from the so-called quadrupolar-induced shifts (δ_{QIS}).[22]

The MQMAS spectrum revealed the presence of at least seven distinguishable boron centers in the sample. The broadening remaining in the multiple-quantum (or isotropic, δ_{ISO}) dimension is mainly due to the distribution of local environments. However, due to strong dependence of the efficiency of MQMAS intensities on the quadrupole coupling, the spectra are non-quantitative in the isotropic dimension and have distorted lineshapes in the directly observed, single-quantum dimension (δ_2). Therefore, we used the MQMAS spectrum to determine the number of different centers and to measure their line shape parameters (δ_{CS} and the so-called second order quadrupolar effect parameter P_Q, see footnote in Table 2), whereas the relative intensities were determined by deconvolution of 1D MAS spectrum (see Fig. 1a), which is quantitative. Since the 1D MAS spectrum was very convoluted in the upfield spectral region, only the combined relative intensity of centers E, F G and H could be reliably estimated.

The minor species B and C (δ_{CS} = 2.9 and 1.2 ppm) with intermediate symmetry (P_Q's between 0.4 and 0.8 MHz) are yet to be assigned. The majority of ^{11}B nuclei resonate at $\delta_{CS} = -5.8$ ppm (centers D, ~15% of total) and between −7.4 and −12.9 ppm (centers E/F/G/H, ~63% of total). The species resonating at −5.8 ppm is highly symmetric as determined by the P_Q value of ~0, whereas those at −7.4, −8.7 and −11.3 ppm have substantial contributions due to quadrupolar interaction (P_Q = 1.8, 1.5 and 1.2 MHz, respectively), indicating low symmetry boron environments. Based on the ^{11}B chemical shifts observed in solution, we postulate that the resonance at $\delta_{CS} = -5.8$ ppm represents *O*-coordinated boron centers and the resonances between −7.4 and −12.9 ppm are attributed to *N*-coordinated boron centers, as depicted in Fig. 1d.

The above assignments are further substantiated by the solid-state ^1H-^{11}B HETCOR spectrum shown in Fig. 1c, which clearly shows that center D is more strongly correlated with CH_2 protons than centers E and F (compare slices 1 and 2 in Fig. 1c). The diversity of chemical shifts observed for the nitrogen-coordinated boron (centers E, F, G and H) is most likely due to various combinations of monomeric units in linear and/or cyclic oligomeric structures that cannot be identified without further studies. Under such a scenario, species A resonating at 22 ppm could represent the end groups of the linear oligomers. Thus, we conclude that **1** is best described as an oligomeric mixture of *N*- and *O*-coordinated $[PhB(Ox^{Me2})_2]_n$ species. Assuming that the linear structure prevails, the average value of n is around 12 based on the measured concentration of A.

The bifunctional borane **1** is stable in the solid state at room temperature for several months when kept under an inert atmosphere. In non-polar and non-coordinating solvents such as benzene-d_6, $PhB(Ox^{Me2})_2$ is the only species observed by ^1H NMR spectroscopy (as broad resonances) after three days. However, thermolysis at 80 °C produces small amounts (*ca.* 5%) of 2H-Ox^{Me2} and unidentified boron-containing products after 12 h. Decomposition is much faster in acetonitrile-d_3 and methanol-d_4, as a small amount of 2H-Ox^{Me2} is observed at room temperature after 24 h. The formation of 4,4-dimethyl-2-oxazoline is accelerated upon heating to 60 °C. This thermal instability, as well as the affinity of $PhB(Ox^{Me2})_2$ for both electrophiles and nucleophiles, has hindered our ability to obtain materials that give satisfactory combustion analysis. However, the species obtained is sufficiently pure for the chemistry described below.

Although **1** appears to be a mixture of linear and cyclic oligomeric species, further derivatization reactions support its identity as a borane. For example, the boron center in **1** is expected to be a reasonably strong Lewis acid due to the electron-withdrawing nature of the 2-oxazoline substituents. Addition of *tert*-butylisocyanide to **1** gives the adduct **1**·CN^{t}Bu in benzene-d_6; this adduct could not be isolated because dissociation of CN^{t}Bu occurs to reform **1** upon evaporation of the solvent. However, the infrared spectrum of a benzene-d_6 solution of this material contains a ν_{CN} band at 2280 cm^{-1} (*cf*. the ν_{CN} of uncoordinated CN^{t}Bu is 2140 cm^{-1} which was not detected in solutions of the adduct). This stretching frequency compares to $Me_3B{\cdot}CN^tBu$ (2247 cm^{-1}), $Ph_3B{\cdot}CN^tBu$ (2272 cm^{-1}) and $(F_5C_6)_3B{\cdot}CN^tBu$ (2310 cm^{-1}),[25] suggesting that borane **1** is a slightly stronger Lewis acid than BPh_3. Additional evidence supporting the identity of **1** is its reaction with 2Li-Ox^{Me2} which gives the previously reported Li[To^M][18] after 12 h (eq. 5).

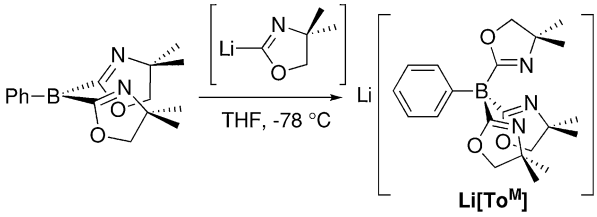

(5)

However the reaction of 2Li-Ox^{Me2} and **1** is slow, and this is likely due to the steric bulk of the oxazoline groups bonded to boron and the intermolecular interactions that form the complicated oligomeric species $[PhB(Ox^{Me2})_2]_n$ described above. Additionally, 2Li-Ox^{Me2} is a relatively weak base (and is weakly

nucleophilic) since 2H-Ox^{Me2} can be deprotonated by bases as weak as LiN(SiMe$_3$)$_2$ (pK_a = 25.8).[26]

Aluminum methyl group abstraction by [PhB(Ox^{Me2})$_2$]

Since borane **1** contains both Lewis basic coordinating groups (*O* and *N* centers in the oxazoline ring) and a Lewis acid boron center, this compound is appropriate for Lewis acid-mediated abstraction/Lewis base coordination. The intermolecular boron-oxazoline interactions are labile, suggesting that both sites are accessible, so with this idea in mind we investigated the interaction of **1** with (AlMe$_3$)$_2$.

In a microliter scale experiment, PhB(Ox^{Me2})$_2$ and 0.5 equiv. of (AlMe$_3$)$_2$ react to initially give a mixture of minor products and [(κ^2-PhMeB(Ox^{Me2})$_2$)AlMe$_2$] (**2**). The reaction continues over a 24 hour period to give the major product with trace amounts of **1** (eq. 6).

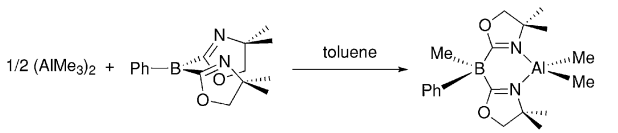

(6)

[(κ^2-PhMeB(Ox^{Me2})$_2$)AlMe$_2$]
(**2**)

On a larger scale, zwitterionic **2** is isolated as a pure white solid after crystallization from toluene. The Al-Me abstraction, mediated by **1**, demonstrates that the borane is a stronger Lewis acid than aluminum(III) in (AlMe$_3$)$_2$. Compound **2** has C_s symmetry, as determined by its ^{1}H NMR spectrum (benzene-d_6). Two upfield singlets (–0.27 and –0.33 ppm, 3 H each) were assigned to inequivalent aluminum methyl groups. Evidence for methyl group abstraction from aluminum by the boron center was provided by a broad resonance in the ^{1}H NMR spectrum at 0.89 ppm (3 H). This signal was unequivocally assigned as a B-CH$_3$ by its crosspeak with a borate resonance (–16.7 ppm) by a ^{1}H-^{11}B HMQC experiment. Coordination of the oxazoline nitrogen to aluminum is indicated by the chemical shift for the oxazoline nitrogen at –186.7 ppm, a change of 59.2 ppm from free H-Ox^{Me2}. The 2D ^{15}N NMR experiment can be extremely powerful for assigning the solution structures of nitrogen containing ligands on transition metal centers.[17,27] Indeed, bonding of the nitrogen to aluminum in **2** was demonstrated by a ^{1}H-^{15}N HMBC experiment, which contained a crosspeak between Al*Me* resonances and the *N*-oxazoline resonance. Crosspeaks corresponding to the expected ^{1}H-^{15}N coupling within the oxazoline ring were also observed. This 2D ^{1}H-^{15}N NMR experiment unambiguously excludes *O*-oxazoline coordination to the oxophilic aluminum. Relatively few measurements of inter-ligand, through-bond ^{15}N-X coupling involving nitrogen-containing ligands at natural abundance have been previously described.[28]

Colorless crystals of **2** are obtained from a concentrated toluene solution cooled to –35 °C for several days, and a single crystal X-ray diffraction study confirms the identity of **2** as [(κ^2-PhMeB(Ox^{Me2})$_2$)AlMe$_2$] (see the ORTEP diagram illustrated in Fig. 2). This structure also provides support for the identity of **1**, as it is a derivative of that compound. Two notable structural features are the planar six-membered BC$_2$N$_2$Al chelate ring and the twisted oxazoline rings that result in a C_1-symmetric solid-state structure.

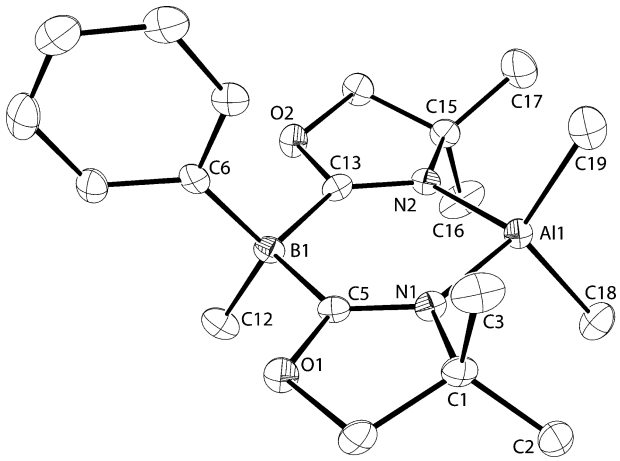

Fig. 2 ORTEP diagram of [(κ^2-PhMeB(Ox^{Me2})$_2$)AlMe$_2$] (**2**) drawn at 35% probability. Hydrogen atoms are excluded for clarity. Relevant bond distances (Å): Al1-N2, 1.918(5); Al1-N1, 1.931(5); Al1-C19, 1.931(8); Al1-C18, 1.986(7); B1-C13, 1.612(8); B1-C6, 1.621(9). Relevant bond angles (°): N2-Al1-N1, 98.4(2); C19-Al1-C18, 116.7(3); C13-B1-C6, 109.5(5).

The torsion angles between co-facial oxazoline C-CH$_3$ vectors on rings 1 and 2 (C2-C1-C15-C16 = 44.48°; C3-C1-C15-C17 = 44.18 °) reveal that the oxazoline groups are twisted to place the methyl groups in pseudo-axial (C3 and C16) and pseudo-equatorial (C2 and C17) positions. This twist is clearly evident in the ORTEP diagram in Fig. 2. The pseudo-axial oxazoline methyl groups are much farther from the plane defined by Al1, C5, and C13 (described below) at 1.75 Å (C3-plane distance) and 1.83 Å (C16-plane distance) than the pseudo-equatorial distances 0.60 Å (C2-plane) and 0.44 (C17-plane). Note that the pseudo-axial methyl groups are located on opposite faces of the complex (disposed in an *anti* fashion), and the torsion angle between the two axial methyl groups and the oxazoline carbon (C3-C1-C15-C16) is 161.37°. This twisted structure, that gives axial and equatorial groups on the oxazoline ring (and overall C_1 symmetry), is not observed in room temperature ^{1}H NMR spectra, where *syn* methyl groups are equivalent (C_s symmetry).

A second interesting structural feature of [(κ^2-PhMeB(Ox^{Me2})$_2$)AlMe$_2$] involves the six-membered chelate ring. The conformation of the chelate ring affects the relative position of the metal center and oxazoline substituents. Additionally, the chelate ring conformation may provide insight into the nature of the bonding interaction of bis(oxazolinyl)borate ligands and a metal center in comparison to pyrazolylborate and bis(oxazoline) ligands. The sum of the six-membered BC$_2$N$_2$Al ring's internal angles is 719.4(3); thus the ring is planar (*cf*. the sum of the internal angles of a perfect planar six-membered ring is 720°). The two C=N are nearly co-planar, as indicated by the torsion angles C5-N1-N2-C13 and N1-C5-C13-N2 of 7.08 and 7.82°. Additionally, the boron center is located in the plane defined by Al1, C5, and C13 atoms in the ring (within error); the two nitrogen atoms, N1 and N2, are displaced by +0.07 and –0.11 Å, respectively, from the same plane but located on opposite sides. The aluminum methyl groups are equidistant from this plane (C18, 1.67 Å; C19, 1.66 Å). For comparison, the structure of {BOX-Me$_2$}AlCl$_2$ contains a similarly planar 6-membered C$_3$N$_2$Al ring. In that case, a delocalized π system favors the planar conformation.[9]

Table 3 Bond distances and angles from X-ray structures and DFT calculations

	$(PhMeB(Ox^{Me2})_2)AlMe_2$ (**2**; X-ray)	$(Me_2B(Ox^{Me2})_2)AlMe_2$ (**X**; B3LYP)	$Bp^{tBu,Me}AlMe_2$ (X-ray)[12]	$(H_2B(N_2C_3H_2)_2)AlMe_2$ (**Z**; B3LYP)
Al-N (Å)	1.918(5), 1.931(5)	1.951	2.0060(4), 1.9868(3)	1.968
N-Al-N (°)	98.4(2)	97.25	102.22	92.94
C-B or N-B (Å)	1.621(9), 1.621(8)	1.619	1.5536(2), 1.5499(2)	1.569
E-B-E (°)	109.5(5)	110.05	109.1	107.34

In contrast, the tetrahedral borate is expected to disrupt π-conjugation in $[(\kappa^2\text{-}PhMeB(Ox^{Me2})_2)AlMe_2]$. X-ray structures of copper(II) borabox compounds contain planar CuN_2C_2B six-membered rings.[7a] Palladium(II) allyl compounds containing borabox adopt planar structures when bonded to the smaller parent $\eta^3\text{-}C_3H_5$ allyl and a boat configuration when bonded to the larger 1,3-diphenylallyl ligand;[7b] this structural change is apparently sterically induced. We have crystallographically characterized several $(\kappa^2\text{-}To^M)IrL_2$ compounds ($L_2 = \eta^4\text{-}C_8H_{12}$ or $(CO)_2$), and in all cases the six-membered BC_2N_2Ir rings form a boat conformation.[29] Thus, planar bis(oxazolinyl)borato chelate rings are formed in the absence of unfavorable interligand steric effects.

This planar ring structure is distinct from related pyrazolylborate aluminum compounds, which form non-planar puckered six-membered rings upon chelation. The cause for the difference between oxazolinylborate and pyrazolylborate conformations is not immediately apparent. Several κ^2-pyrazolylborate aluminum(III) compounds have been crystallographically characterized, and they adopt boat configurations with the borate center significantly displaced from a plane defined by the four nitrogen centers.[11-13] For example, the sum of the internal angles of the BN_4Al ring in $Bp^{tBu,Me}AlMe_2$ is 680° ($Bp^{tBu,Me} = H_2B(3\text{-}^tBu\text{-}5\text{-}Me\text{-}N_2C_3H)_2$).[12] This puckered geometry was noted by Trofimenko early in pyrazolylborate chemistry and attributed to constraints imposed by the B-N and M-N bond lengths and angles.[30] However, the Al-N and B-N bond angles and distances in $[Bp^{tBu,Me}AlMe_2]$ are reasonably similar to the Al-N and B-C bond distances and angles in **2** (see Table 3). It seems unlikely that these values are sufficiently different to rationalize the configurational differences in $[Bp^{tBu,Me}AlMe_2]$ and $[(\kappa^2\text{-}PhMeB(Ox^{Me2})_2)AlMe_2]$ as resulting from ring strain. This conclusion is supported by density functional theory (DFT) calculations, which reproduce the planar and boat conformations for bis(oxazolinyl)borato- and bis(pyrazolyl)borato-aluminum dimethyl, respectively, with very similar B-C, B-N, and Al-N bond distances (see below).

A second possible explanation for the different structures involves unfavorable interligand steric interactions between aluminum methyl groups and the phenyl and methyl substituents on boron. The dialuminum pyrazolyl compounds $^tBu_2Al(\mu\text{-}N_2C_3H_2)_2Al^tBu_2$ and $Me_2Al(\mu\text{-}N_2C_3Me_2H)_2AlMe_2$ are planar,[31] and this is attributed to steric interactions. In compound **2**, the shortest C-C distance between the phenyl substituent on boron and methyl aluminum is long (C-C = 4.76 Å); additionally, space filling models show no close contacts between the aluminum methyls and boron substituents. The steric properties of the ligands in **2** were further evaluated using solid angles;[32] this method treats the metal center as a point source of light and the ligands cast shadows on a sphere surrounding the complex. The surface area of the shadow produced by the $PhMeB(Ox^{Me2})_2$ ligand is 6.14 steradians, corresponding to 48.9% of the space surrounding the aluminum center (determined with the program *Solid-G*).[33] There are no unfavorable interligand interactions in $[(\kappa^2\text{-}PhMeB(Ox^{Me2})_2)AlMe_2]$.

DFT calculations of model compounds were used to further investigate these compounds' configurations. The 4,4-disubstituted oxazoline compound $[\kappa^2\text{-}Me_2B(Ox^{Me2})_2)AlMe_2]$ (**X**) was calculated as a model for **2** (see Fig. 3), and $[Bp^{tBu,Me}AlMe_2]$ was modeled with $[(\kappa^2\text{-}H_2Bpz_2)AlMe_2]$ (**Z**). In all geometry optimization attempts, a planar structure is obtained with the oxazolinylborate compound while the pyrazolylborate compounds provided the same puckered boat configuration observed experimentally. The Al-N, B-N and B-C bond distances and angles for model compound **X** are similar to the values observed by X-ray crystallography for compound **2** (see Table 3).

An electronic difference between oxazoline and pyrazole groups might be responsible for the two different configurations, especially since the sterically unhindered transition metal compounds of bis(oxazolinyl)borate are planar. Indeed, the Kahn-Sham orbitals, obtained from the DFT calculations and shown in Fig. 3, support this notion. The HOMO and the HOMO–2 orbitals of **X** and of **Z** are similar in appearance. As expected, the HOMO of the two model compounds primarily involves aluminum-methyl bonding. The HOMO–2 of **X** and **Z** are composed of p-orbitals, and the important lobes are on the nitrogen bonded to aluminum. As can be seen from Fig. 3, the lobes on the two rings are out of phase, and the puckered distortion from planarity increases unfavorable antibonding interactions between the two oxazoline or two pyrazolyl rings. Since these nitrogen centers are far apart (2.85 Å), the importance of this interaction is likely to be minimal in the absence of extreme distortion. The substantial difference between **X** and **Z** is found in the HOMO–1 orbital. This orbital corresponds primarily to the B-C bonds in the oxazolinylborate model. In contrast, the pyrazolylborate model contains significant electron density located on the nitrogen bonded to boron as well as lobes corresponding to B-H bonds. The out-of-phase interaction between the nitrogen p orbitals and the B-H σ-bonds is unfavorable, and a boat conformation minimizes this interaction.

Comparisons between bis(oxazolinyl)borate and tris(oxazolinyl)borate aluminum compounds

We were interested in comparing aluminum compounds derived from the abstraction-based proligand **1** to the (potentially) tridentate To^M aluminum(III) compound obtained by methyl-group protonolysis. In benzene-d_6, reaction of $H[To^M]$ and 0.5 equiv. of $(AlMe_3)_2$ affords $[(\kappa^2\text{-}To^M)AlMe_2]$ (**3**) and CH_4.

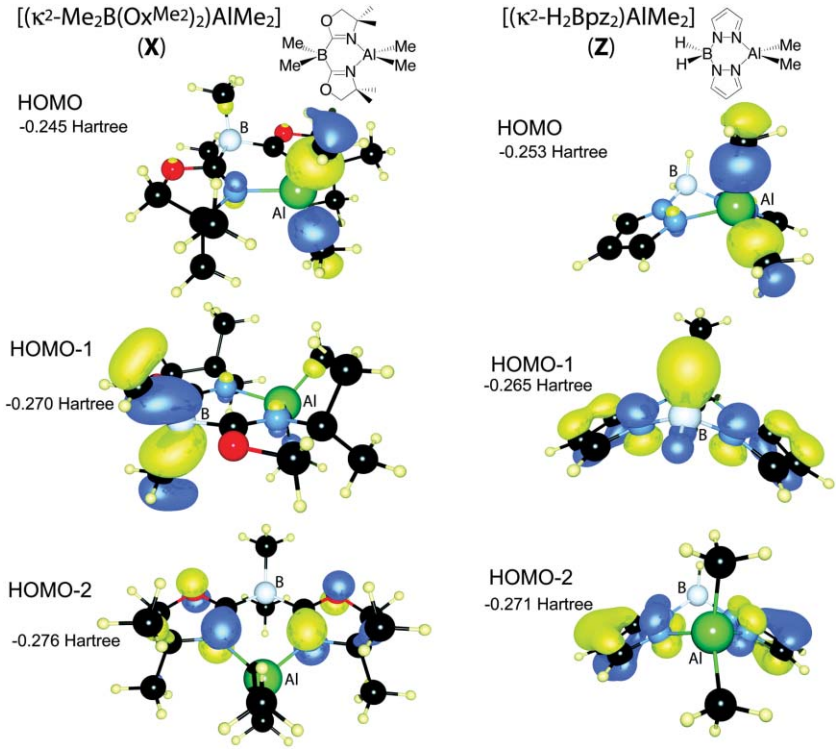

Fig. 3 Kahn-Sham orbitals for $[(\kappa^2\text{-}Me_2B(Ox^{Me2})_2)AlMe_2]$ (**X**) and $[(\kappa^2\text{-}H_2Bpz_2)AlMe_2]$ (**Z**) obtained from DFT calculations showing a) the HOMO, b) the HOMO–1, and c) the HOMO–2.

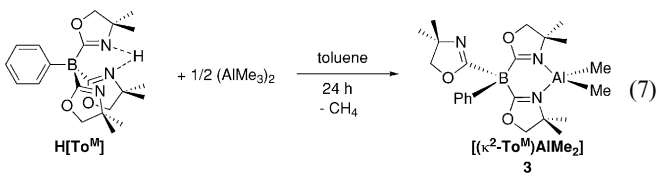

(7)

The ^{1}H NMR spectrum of the resulting compound was consistent with a C_s symmetric structure. Three singlets are observed for the oxazoline methyls, and the methylene groups appear as two diastereotopic doublets and a singlet. The aluminum methyl groups are inequivalent. Bidentate coordination is confirmed by a ^{1}H-^{15}N HMBC (Fig. 4), which shows coupling between the aluminum methyl moieties and nitrogens that are also coupled to diastereotopic doublets. The ^{15}N NMR chemical shifts of the non-coordinated oxazoline (–120.2 ppm) is close to that of 4,4-dimethyl-2-oxazoline (–127.5 ppm), whereas the *Al*-coordinated oxazoline nitrogens have a chemical shift of -184.2 ppm.

Although To^M is coordinated to aluminum in a bidentate fashion in **3**, crosspeaks in an EXSY experiment showed that the three oxazoline groups undergo slow exchange on the ^{1}H NMR timescale at room temperature. At elevated temperature, the oxazoline resonances in the ^{1}H NMR spectrum in toluene-d_8 were broadened and moved closer together, but did not coalesce at 370 K.

Attempts to coordinate the third oxazoline by abstraction or protonolytic elimination of a methyl group with $B(C_6F_5)_3$ or $[HNMe_2Ph][BPh_4]$ were unsuccessful. For example, addition of 1 equiv. of $[HNMe_2Ph][BPh_4]$ to **3** in THF-d_8 at room temperature gives the cationic compound $[PhB(Ox^{Me2}H)(Ox^{Me2})_2AlMe_2]$ (**4**), where the pendent oxazoline is protonated rather than an aluminum methyl. Evidence for oxazoline protonation includes a downfield signal at 10.94 ppm in the ^{1}H NMR spectrum assigned to the NH and a ^{1}H-^{15}N HMQC experiment that showed a crosspeak between this resonance and the peak representing the oxazoline nitrogen (–202.8 ppm). This chemical shift is far upfield by 82 ppm of the pendent oxazoline in **3** (–120.2 ppm). Interestingly, the ^{15}N NMR chemical shifts of the aluminum-bonded nitrogen do not change significantly (**3**: –184.2 *vs* **4**: –176.9 ppm). Exposure of **3** to two equivalents of the anilinium salt results in the same protonated species with no evidence of a second product over a 48 hour period.

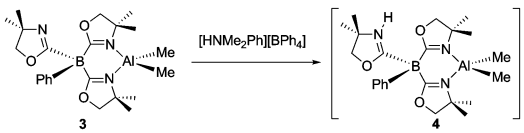

(8)

Although ligand-based protonations for pyrazolylborates and oxazolinylborates have been previously reported,[34] the site of protonation varies between ligand and metal center even within isoelectronic and isostructural compounds. For example, $[Tp^*Rh(CO)_2]$ and $HBF_4{\cdot}OEt_2$ gives a protonated pyrazole compound $[HB(pz\text{-}H)(pz)_2Rh(CO)_2]BF_4$, but protonation of $[Tp^*Ir(CO)_2]$ gives the iridium hydride $[Tp^*IrH(CO)_2][BF_4]$.[34a] We have previously reported that iridium compounds $[Ir(To^P)(\eta^4\text{-}C_8H_{12})]$, $[Ir(To^P)(CO)_2]$, and $[Ir(To^M)(CO)_2]$ react with strong acids (such as HOTf) to afford oxazoline protonation rather than formation of a metal hydride.[17,29] The exclusive reaction at the pendent oxazoline described here, however, is unexpected given the relatively strong nucleophilic character of Al-Me groups. Additionally, we expected that intra- or intermolecular proton

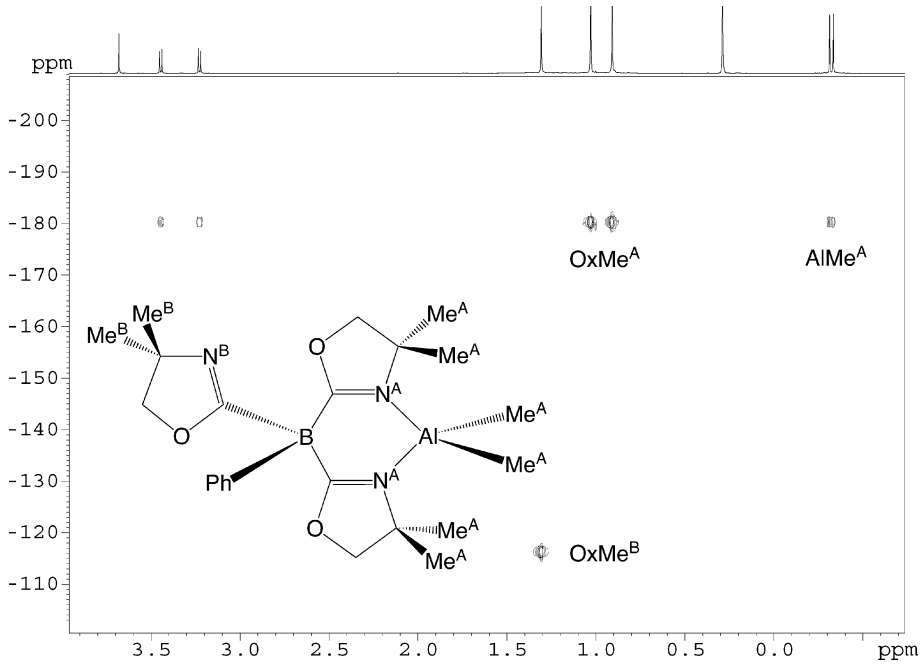

Fig. 4 ^{1}H-^{15}N HMBC experiment illustrating three bond coupling between the oxazoline nitrogen through aluminum to the methyl group in [(κ^2-To^M)AlMe$_2$] (**3**).

transfer from the oxazolinium to an aluminum methyl would occur over time. Since the oxazoline groups in the precursor **3** undergo slow exchange (as observed with an EXSY experiment) the pendent oxazolinium must have some access to the aluminum center. Coordination of three bulky, non-planar 4,4-dimethyl-2-oxazolinyl groups to a small aluminum(III) center (4-coordinate radius is 0.39 Å)[35] is clearly sterically unfavorable. Over an extended time (*ca.* 1 month), compound **4** decomposes to form H[To^M]. This process is accelerated thermally; thus thermolysis of **4** at 100 °C gives H[To^M], methane, and unknown aluminum-containing material after 48 h.

The inert nature of the aluminum-methyl bonds in **3** toward protonolysis does not depend on the presence of a pendant oxazoline group. Bis(oxazolinyl)borate **2** shows similar resistance toward protonolysis of the aluminum methyl. Thus, only starting materials were observed in ^{1}H NMR spectra of reaction mixtures of [(κ^2-PhMeB(Ox^{Me2})$_2$)AlMe$_2$] and [NHMe$_2$Ph][BPh$_4$] after 48 h in THF-d_8 at room temperature. In terms of their reactivity with acids, the contrast between oxazolinylborate aluminum compounds **2** or **3** and carbon-bridged, π-delocalized monoanionic {BOX-Me$_2$}AlMe$_2$ compounds is striking. The latter compound, as well as the optically active compound {BOX-(*S*)-^{i}Pr}AlMe$_2$, is reported to react rapidly with B(C$_6$F$_5$)$_3$ to give {BOX-Me$_2$}AlMe][MeB(C$_6$F$_5$)$_3$],[9] whereas **2** gives complicated mixtures (in benzene-d_6, bromobenzene-d_5, and tetrahydrofuran-d_8) upon addition of B(C$_6$F$_5$)$_3$. One possible explanation for the reticence of **2** and **3** to react with acids to form cationic compounds (with the charge centered on the metal) is that the oxazolinylborato aluminum compounds are zwitterionic, and formation of a cationic compound would further exacerbate the charge separation. This explanation is supported by the Mulliken charges calculated for model compound **X**, which give boron a negative charge (–0.398) and aluminum a positive charge (+0.267).

Lactide polymerization with oxazolinylboratoaluminum compounds

These oxazolinylboratoaluminum compounds are thermally robust and resistant toward hydrolysis, and these properties suggest that they might be useful in catalytic processes that require relatively high temperatures. Because catalytic lactide ring-opening polymerizations occur in neat liquid lactide at temperatures greater than 110 °C, this transformation is a good initial trial reaction. Additionally, a number of well-defined aluminum compounds are well known as catalysts for lactide ring-opening polymerizations.[36,37]

Our first experiments with compound **3** in NMR scale reactions demonstrated that lactide is catalytically consumed at 110 °C (toluene-d_8, 20:1 lactide:catalyst ratio), as resonances in the ^{1}H NMR spectrum corresponding to lactide decreased in intensity and broad resonances assigned to polylactic acid emerged.

Compound **3** was then investigated as a catalyst for polymerization of lactide (Table 4). In general, the catalyst was mixed with lactide, sealed in an ampoule, and heated from 110-130 °C. At 130 °C, 90% conversion of monomer occurs after 24 h as determined by integration of a ^{1}H NMR spectrum of the crude reaction mixture (entry 8). Significantly lower conversion (46%) occurs at 110 °C after 24 h (entry 5), but over longer reaction times (48 h and 72 h, entries 5 and 7, respectively) conversion is increased. This suggests that the catalyst remains active over the course of the polymerization experiment. Analysis of the polymer's molecular weight (M_w and M_n) and polydispersity (PDI) with gel permeation chromatography reveals that averaged molecular weights unexpectedly decrease with increased conversion, and at the same time the polydispersity is narrowed (entries 5-7). Additionally, the polydispersity increased with decreasing temperature.[38] The GPC traces indicate that the polymer distributions are monomodal; thus it appears likely that there is a single active site present. Thus,

Table 4 Polymerization of *rac*-lactide using [(κ²-To^{M})AlMe$_2$] (**3**)[a]

Entry	*rac*-LA:Al	Time (h)	Conversion (%)[b]	Yield (%)[c]	$M_{n,th}$[d]	M_n	M_w	PDI
1	100:1	24	80	39	11 500	28 200	44 300	1.57
2	100:1	48	100	85	14 400	26 600	45 000	1.69
3	200:1	24	60	38	17 300	33 500	56 900	1.70
4	200:1	48	88	62	25 300	44 400	68 900	1.55
5	500:1	24	46	34	33 100	39 500	68 400	1.73
6	500:1	48	61	53	43 900	31 400	51 100	1.63
7	500:1	72	90	64	64 800	27 600	40 000	1.45
8[e]	500:1	24	90	87	64 800	26 200	41 300	1.57

[a] Standard conditions: lactide and **3** are sealed in ampoules and heated at 110 °C. [b] Conversion is determined by integration of the ^{1}H NMR spectrum of the crude reaction mixture. [c] Yield is calculated as the ratio of the mass of isolated polymer versus the mass of the starting monomer. [d] Theoretical M_n calculated from molecular weight of lactide × conversion × [LA]/[Al]. [e] Polymerization experiment at 130 °C.

Table 5 Comparison of aluminum catalysts for *rac*-lactide polymerization[a]

Entry	Catalyst	Conversion (%)[b]	Yield (%)[c]	$M_{n,th}$[d]	M_n	M_w	PDI
1	PhMeB(Ox^{Me2})$_2$AlMe$_2$ (**2**)	82	42	59 000	10 300	13 900	1.34
2	To^{M}AlMe$_2$ (**3**)	90	87	64 800	26 200	41 300	1.57
3	To^{M}Al(O^{i}Pr)$_2$ (**5**)	86	48	61 900	9 600	15 800	1.63
4	To^{P}AlMe$_2$ (**6**)	87	39	62 600	28 700	44 600	1.55

[a] Polymerization experiments are performed in sealed ampoules in neat lactide at 500:1 lactide:catalyst for 24 h at 130 °C. [b] Conversion is determined by integration of the ^{1}H NMR spectrum of the crude reaction mixture. [c] Yield is calculated as the ratio of the mass of isolated polymer *versus* the mass of the starting monomer. [d] Theoretical M_n calculated from molecular weight of lactide × conversion × [LA]/[Al].

the pendent oxazoline and aluminum centers are not acting as independent catalysts.

Higher catalyst loading results in greater conversion of monomer (*cf*. entries 1, 3, and 5) at equal times. Although the samples' polydispersity generally improve with increased conversion, the polymers' chain lengths are shorter as represented by M_n and M_w values. The polydispersities (PDI) obtained are higher than those from other aluminum catalysts, though not significantly.[36]

Thus, other oxazolinylboratoaluminum compounds were investigated for lactide polymerization. In particular, compounds **2** and **3** were compared as catalysts and found to have significantly different activities (see Table 5, entries 1 and 2). While approximately the same conversion of lactide occurs after 24 h, the molecular weights and polymer yield obtained with the tris(oxazolinyl)borate **3** are significantly higher than obtained with the bis(oxazolinyl)borate **2**.

Given this unexpectedly significant difference, two other oxazolinylboratealuminum complexes were prepared and tested in lactide polymerization. We synthesized an aluminum alkoxide compound [(κ²-To^{M})Al(O^{i}Pr)$_2$] (**5**) by reaction of H[To^{M}] with Al(O^{i}Pr)$_3$. Although Al(O^{i}Pr)$_3$ is a well-known initiator for aluminum-catalyzed lactide polymerization,[36] poly(lactide) obtained when compound **5** was the catalyst had substantially shorter chain lengths as well as a broader molecular weight distribution (Table 5, compare entries 2 and 3).

Additionally, we were interested in attempting stereo-controlled polymerization using the chiral analogue [(κ²-To^{P})AlMe$_2$] (**6**). Compound **6** was synthesized *via* the reaction of H[To^{P}] and (AlMe$_3$)$_2$. The ^{1}H NMR spectrum of **6** reveals its C_1 symmetric solution structure; thus, six sets of isopropyl methyls were observed (all oxazoline rings are inequivalent). Interestingly, in the ^{13}C{^{1}H} NMR spectrum, four isopropyl methyl carbons are overlapping, and only two signals for these are observed. A ^{1}H-^{13}C HMQC experiment permitted the assignment of these overlapping resonances. The chiral catalyst **6** and achiral catalyst **3** give remarkably similar poly(lactide) yields, molecular weights, and polydispersities. Unfortunately, the achiral and chiral catalysts both produce atactic polymer microstructures, as determined by ^{13}C{^{1}H} NMR spectroscopy.[39] Although the polydispersity and molecular weights are consistent with other aluminum catalysts,[37] the deviations in conversion *versus* molecular weight indicate that catalysis is complicated, and we are currently investigating the polymerization mechanism with respect to catalyst activation, conversion, and molecular weights.

Conclusion

The title compound bis(4,4-dimethyl-2-oxazolinyl)phenylborane (**1**) exists as a mixture of oligomers, in which the monomers are connected by *O*- and *N*-oxazoline coordination to an adjacent Lewis acidic boron center. The spectroscopic data, including through-space solid-state ^{1}H-^{11}B HETCOR and ^{11}B MQMAS experiments, are consistent with this complicated structure. Despite the coordination of oxazolines or solvent to the boron centers that might have inhibited its reactivity, **1** is sufficiently Lewis acidic to abstract a methyl group from trimethylaluminum and coordinate the oxazolines to the aluminum center giving the zwitterionic oxazolinylboratoaluminum complex **2**.

This strategy, involving Lewis acid-mediated abstraction to give zwitterionic organometallic compounds, is potentially valuable for the preparation of new catalysts, especially since the activation of transition metal centers often involves formation of cationic complexes. Furthermore, oxazoline-based ligands are important

in asymmetric catalysis. In this respect, the aluminum compounds investigated here have shown activity in lactide ring-opening polymerization, giving relatively high molecular weight polymers with low polydispersities in the range of other aluminum catalysts. Our limited investigation of one chiral oxazolinylboratoaluminum compound has not provided a stereoregular polymer. However, this does not rule out further investigations in stereoselective processes since the steric and electronic properties of these ligands can be varied through modification of the oxazoline group.

Experimental

General

All manipulations were performed using either Schlenk techniques, or in a glovebox under an inert atmosphere of nitrogen unless otherwise indicated. Dry, oxygen-free solvents were used throughout. Benzene, toluene, methylene chloride, pentane, diethyl ether, and tetrahydrofuran were degassed by sparging with nitrogen, filtered through activated alumina columns, and stored under N_2. Dichlorophenylborane was purchased from Aldrich and distilled prior to use. Trimethyl aluminum, aluminum isopropoxide, and 3,6-dimethyl-1,4-dioxane-2,5-dione were purchased from Aldrich and used as received. 4,4-dimethyl-2-oxazoline was purchased from Acros and used as received. Hydrogen tris(4,4-dimethyl-2-oxazolinyl)phenylborate (H[To^M])[18] and hydrogen tris(*4S*-isopropyl-2-oxazolinyl)phenylborate (H[To^P])[17] were prepared as previously reported. The anilinium salt [HNMe$_2$Ph][BPh$_4$] was prepared *via* reaction of *N*,*N*-dimethylaniline, sodium tetraphenylborate, and hydrochloric acid.

Solution ^{1}H, ^{13}C{^{1}H}, and ^{11}B NMR spectra were collected on a Bruker DRX-400 spectrometer, and ^{15}N chemical shifts were determined by ^{1}H-^{15}N HMBC experiments on a Bruker Avance II 700 spectrometer with a Bruker Z-gradient inverse TXI ^{1}H/^{13}C/^{15}N 5 mm cryoprobe. ^{15}N chemical shifts were originally referenced to liquid NH_3 and recalculated to the CH_3NO_2 chemical shift scale by adding −381.9 ppm. ^{11}B NMR spectra were referenced to an external sample of $BF_3{\cdot}Et_2O$.

Solid-state ^{11}B MAS, ^{11}B MQMAS and ^{11}B-^{1}H HETCOR NMR spectra were measured at 599.7 (^{1}H) and 192.4 (^{11}B) MHz on a Varian NMR System 600 spectrometer equipped with a doubly tuned Varian FastMAS(tm) probe. Approximately 7 mg of [PhB(Ox^{Me2})$_2$] was loaded into 1.6 mm zirconia rotor under oxygen-free atmosphere and tightly capped. The T_1 relaxation times were determined to be 0.9 s for ^{1}H and 2.4 s for ^{11}B nuclei using the inversion recovery method. Other experimental conditions are given in the caption to Fig. 1, where B_0 denotes the static magnetic field, ν_R the MAS rate, ν^H_{RF} and ν^B_{RF} the magnitudes of radiofrequency magnetic fields applied to ^{1}H and ^{11}B spins, τ_{CP} the cross polarization time, τ_{RD} the recycle delay, NS the number of scans and AT the total acquisition time.

Elemental analysis was performed using a Perkin-Elmer 2400 Series II CHN/S by the Iowa State Chemical Instrumentation Facility. X-ray diffraction data was collected on a Bruker-AXS SMART 1000 CCD diffractometer using Bruker-AXS SHELXTL software. Gel permeation chromatography (GPC) measurements were performed on a Viscotek GPC Max 280 separation module equipped with three 5 μm I-gel columns connected in series (guard, HMW, MMW and LMW) with a refractive index detector. Analyses were performed at 35 °C using THF as the eluent, and the flow rate was 1.0 mL/min. Calibration was based on polystyrene standards obtained from Viscotek.

[PhB(Ox^{Me2})$_2$] (1)

A 100 mL Schlenk flask was charged with 4,4-dimethyl-2-oxazoline (1.0 mL, 9.48 mmol), which was then degassed by three freeze–pump–thaw cycles. The degassed oxazoline was dissolved in 50 mL of tetrahydrofuran and the flask was cooled to -78 °C. Using a syringe, 2.5 M *n*-BuLi (4.0 mL, 10.0 mmol) was added to the cold solution and the resultant solution was stirred for 45 min at -78 °C. Dichlorophenylborane (0.619 mL, 4.72 mmol) was added dropwise *via* syringe into the flask and the solution was stirred for 1 h at -78 °C. Then, the solution was allowed to gradually warm to room temperature. After stirring for 14 h at room temperature, the solvent was removed under reduced pressure to afford a light yellow solid. The resulting solid was extracted with benzene, and the solvent was removed *in vacuo* to yield PhB(Ox^{Me2})$_2$ as a yellow solid (1.27 g, 4.47 mmol, 94.3%). ^{1}H NMR (acetonitrile-d_3, 400 MHz): δ 7.42 (d, ^3J = 7.2 Hz, 2 H, *ortho*-C$_6$H$_5$), 7.13 (m, 2 H, *meta*-C$_6$H$_5$), 7.05 (m, 1 H, *para*-C$_6$H$_5$), 3.64 (d, 2 H, $^2J_{HH}$ = 8.0 Hz, CNCMe$_2$C*H*$_2$O), 3.57 (d, 2 H, $^2J_{HH}$ = 8.0 Hz, CNCMe$_2$C*H*$_2$O), 1.26 (s, 6 H, CNC*Me*$_2$CH$_2$O), 1.17 (s, 6 H, CNC*Me*$_2$CH$_2$O). ^{13}C{^{1}H} NMR (acetonitrile-d_3, 150 MHz): δ 183.00 (br, *C*NCMe$_2$CH$_2$O), 132.86 (*ortho*-C$_6$H$_5$), 127.58 (*meta*-C$_6$H$_5$), 125.99 (*para*-C$_6$H$_5$), 77.79 (CNCMe$_2$*C*H$_2$O), 67.44 (CN*C*Me$_2$CH$_2$O), 28.71 (CNC*Me*$_2$CH$_2$O). ^{11}B NMR (acetonitrile-d_3, 128 MHz): δ -8.1. ^{15}N{^{1}H} NMR (acetonitrile-d_3, 71 MHz): δ -147.0 (*C*NCMe$_2$CH$_2$O). IR (KBr, cm^{-1}): 3069 w, 3046 w, 2964 s, 2930 s, 2872 m, 1621 s, 1601 s, 1462 s, 1432 s, 1384 m, 1346 w, 1260 s, 1194 s, 1126 m, 1083 w, 993 s, 970 s, 886 m, 703 s. Calcd for C$_{16}$H$_{21}$BN$_2$O$_2$: C, 67.63; H, 7.45, N, 9.86. Found: C, 64.69; H, 7.51; N, 8.26. mp 133–137 °C.

[(κ^2-PhMeB(Ox^{Me2})$_2$)AlMe$_2$] (2)

Compound **1** (1.00 g, 3.52 mmol) was placed in a 100 mL Schlenk flask in the glovebox. The solid was dissolved in 50 mL of toluene, and (AlMe$_3$)$_2$ (0.257 g, 1.78 mmol) was added *via* syringe to give a yellow solution. This solution was stirred for 24 hours and then filtered to remove a white precipitate. The toluene filtrate was evaporated under reduced pressure to give a yellow solid. The crude solid was dissolved in toluene and cooled to -80 °C for 24 hours to give a pale yellow solid (0.674 g, 1.90 mmol, 54%) of suitable purity for further reactions. X-ray quality crystals were grown from a concentrated toluene solution after one week at -35 °C. ^{1}H NMR (benzene-d_6, 400 MHz): δ 7.76 (d, $^3J_{HH}$ = 6.8 Hz, 2 H, *ortho*-C$_6$H$_5$), 7.43 (vt, $^3J_{HH}$ = 7.6 Hz, 2 H, *meta*-C$_6$H$_5$), 7.23 (t, $^3J_{HH}$ = 7.6 Hz, 1 H, *para*-C$_6$H$_5$), 3.23 (d, $^3J_{HH}$ = 9.0 Hz, 2 H, CNCMe$_2$C*H*$_2$O), 3.12 (d, $^3J_{HH}$ = 9.0 Hz, 2 H, CNCMe$_2$C*H*$_2$O), 0.93 (s, 6 H, CNC*Me*$_2$CH$_2$O), 0.92 (s, 6 H, CNC*Me*$_2$CH$_2$O), 0.89 (s br, 3 H, B*Me*), -0.27 (s, 3 H, Al*Me*), -0.33 (s, 3 H, Al*Me*). ^{13}C{^{1}H} NMR (benzene-d_6, 125 MHz): δ 180.5 (br, *C*NCMe$_2$CH$_2$O), 135.6 (*ipso*-C$_6$H$_5$), 132.7 (*ortho*-C$_6$H$_5$), 128.3 (*meta*-C$_6$H$_5$), 126.3 (*para*-C$_6$H$_5$), 79.41 (CNCMe$_2$*C*H$_2$O), 65.26 (CN*C*Me$_2$CH$_2$O), 27.17 (CNC*Me*$_2$CH$_2$O), 26.96 (CNC*Me*$_2$CH$_2$O), 4.76 (br, B*C*H$_3$), -5.53 (br, Al*C*H$_3$). ^{11}B NMR (benzene-d_6, 128 MHz): δ -16.7. ^{15}N

NMR (benzene-d_6, 71 MHz): δ -186.7 (Al(NCMe$_2$CH$_2$OC)$_2$B). IR (KBr, cm^{-1}): 3042 w, 2981 s, 2931 s, 1551 s, 1465 s, 1431 m, 1372 s, 1293 s, 1256 m, 1201 s, 1163 m, 1017 m, 992 s, 828 w, 776 w, 703 s. Anal. Calcd for $C_{19}H_{30}BAlN_2O_2$: C, 64.06; H, 8.49; N, 7.86. Found: C, 63.88; H, 8.49; N, 7.74. mp 150-155 °C, dec.

[(κ^2-To^M)AlMe$_2$] (3)

H[To^M] (1.00 g, 2.61 mmol) was dissolved in 50 mL of toluene, and (AlMe$_3$)$_2$ (0.19 g, 1.32 mmol) was added *via* syringe. The solution was stirred for 24 hours to give a pale yellow solution above a small amount of precipitate. The mixture was filtered and the filtrate was evaporated under reduced pressure to yield a crude white solid. Analytically pure [(κ^2-To^M)AlMe$_2$] (0.95 g, 2.17 mmol, 83%) was obtained by recrystallization from a toluene/pentane mixture. ^{1}H NMR (benzene-d_6, 400 MHz): δ 7.98 (d, $^3J_{HH}$ = 7.5 Hz, 2 H, *ortho*-C$_6$H$_5$), 7.43 (vt, $^3J_{HH}$ = 7.5 Hz, 2 H, *meta*-C$_6$H$_5$), 7.22 (t, $^3J_{HH}$ = 7.5 Hz, 1 H, *para*-C$_6$H$_5$), 3.69 (s, 2 H, CNCMe$_2$C*H*$_2$O), 3.44 (d, $^3J_{HH}$ = 8.9 Hz, 2 H, Al(NCMe$_2$C*H*$_2$OC)$_2$B), 3.21 (d, $^3J_{HH}$ = 8.9 Hz, 2 H, Al(NCMe$_2$C*H*$_2$OC)$_2$B), 1.32 (s, 6 H, CNC*Me*$_2$CH$_2$O), 1.02 (s, 6 H, Al(NC*Me*$_2$CH$_2$OC)$_2$B), 0.90 (s, 6 H, Al(NC*Me*$_2$CH$_2$OC)$_2$B), -0.30 (s, 3 H, Al*Me*), -0.32 (s, 3 H, Al*Me*). ^{13}C{^{1}H} NMR (benzene-d_6, 125 MHz): δ 196.6 (br, *C*NCMe$_2$CH$_2$O), 196.5 (br, *C*NCMe$_2$CH$_2$O), 146.3 (br, *ipso*-C$_6$H$_5$), 134.16 (*ortho*-C$_6$H$_5$), 127.59 (*meta*-C$_6$H$_5$), 126.13 (*para*-C$_6$H$_5$), 79.83 Al(NCMe$_2$*C*H$_2$OC)$_2$B), 77.25 (CNCMe$_2$*C*H$_2$O), 68.04 (CN*C*Me$_2$CH$_2$O), 65.46 (Al(N*C*Me$_2$CH$_2$OC)$_2$B), 29.00 (CNC*Me*$_2$CH$_2$O), 27.07 (Al(NC*Me*$_2$CH$_2$OC)$_2$B), 26.78 (Al(NC*Me*$_2$CH$_2$OC)$_2$B), -5.88 (s, Al*Me*), -5.99 (s, Al*Me*). ^{11}B NMR (benzene-d_6, 128 MHz): δ -16.5. ^{15}N{^{1}H} NMR (benzene-d_6, 71 MHz): -120.2 (*C*NCMe$_2$CH$_2$O), -184.2 (Al(*N*CMe$_2$CH$_2$OC)$_2$B). IR (KBr, cm^{-1}): 3053 m, 2968 s, 2930 s, 2889 s, 1626 s, 1565 s, 1462 s, 1433 m, 1373 s, 1360 s, 1294 s, 1252 m, 1200 s, 1160 s, 1100 s, 973 s, 887 m, 677 s. Anal. Calcd for $C_{23}H_{35}BAlN_3O_3$: C, 62.8; H, 8.03; N, 9.56. Found: C, 62.40; H, 8.15; N, 9.26. mp 155-161 °C.

[(PhB(Ox^{Me2}H)(Ox^{Me2})$_2$)AlMe$_2$][BPh$_4$] (4)

A THF solution of [(κ^2-To^M)AlMe$_2$] (0.150 g, 0.342 mmol) was added to a vial containing [HNMe$_2$Ph][BPh$_4$] (0.158 g, 0.359 mmol). The resulting colorless solution was stirred for 30 min, and then the solvent was removed under reduced pressure. The crude solid [PhB(Ox^{Me2}H)(Ox^{Me2})$_2$AlMe$_2$][BPh$_4$] was washed with pentane to remove dimethylaniline. Analytically pure off-white product (0.167 g, 0.220 mmol, 64%) was obtained by crystallization from a THF/pentane solution at -35 °C. ^{1}H NMR (THF-d_8, 400 MHz): δ 10.94 (s, 1 H, N*H*), 7.26 (m, 8 H, *ortho*-Ph$_4$B), 7.25 (m, 2 H, *ortho*-C$_6$H$_5$), 6.83 (vt, $^3J_{HH}$ = 7.6 Hz, 8 H, *meta*-Ph$_4$B), 6.83 (vt, $^3J_{HH}$ = 7.6 Hz, 2 H, *meta*-C$_6$H$_5$), 6.69 (t, $^3J_{HH}$ = 7.1 Hz, 4 H, *para*-Ph$_4$B), 6.65 (t, $^3J_{HH}$ = 7.1 Hz, 1 H, *para*-C$_6$H$_5$B), 4.27 (s, 2 H, HNCMe$_2$C*H*$_2$OC), 4.21 (d, 2 H, $^3J_{HH}$ = 8.8 Hz, Al(NCMe$_2$C*H*$_2$OC)$_2$B), 4.09 (d, 2 H, $^3J_{HH}$ = 8.8 Hz, Al(NCMe$_2$C*H*$_2$OC)$_2$B), 1.39 (s, 6 H, Al(NC*Me*$_2$CH$_2$OC)$_2$B), 1.37 (s, 6 H, Al(NC*Me*$_2$CH$_2$OC)$_2$B), 1.26 (s, 6 H, CNC*Me*$_2$CH$_2$O), -0.52 (s, 3 H, Al*Me*), -0.92 (s, 3 H, Al*Me*). ^{13}C{^{1}H} NMR (THF-d_8, 125 MHz): δ 190.02 (br, *C*NCMe$_2$CH$_2$O), 165.20 (q, $^2J_{B-C}$ = 49.5 Hz, *ipso*-Ph$_4$B), 137.19 (*ortho*-Ph$_4$B), 135.54 (*ortho*-C$_6$H$_5$), 125.90 (*meta*-C$_6$H$_5$), 125.81 (*meta*-Ph$_4$B), 121.91 (*para*-Ph$_4$B), 121.60 (*para*-C$_6$H$_5$), 84.09 (CNCH$_2$*C*H$_2$O), 81.75 (Al(NCMe$_2$*C*H$_2$OC)$_2$B), 68.22 (CN*C*Me$_2$CH$_2$O), 63.45 (Al(N*C*Me$_2$CH$_2$OC)$_2$B), 27.87 (Al(NC*Me*$_2$CH$_2$OC)$_2$B), 27.13 (Al(NC*Me*$_2$CH$_2$OC)$_2$B), 26.35 (CNC*Me*$_2$CH$_2$O), -6.43 (Al*Me*$_2$), -6.92 (Al*Me*$_2$). ^{11}B NMR (THF-d_8, 128 MHz): δ -7.51 (*B*Ph$_4$), -12.41 (Ph*B*(Ox^{Me2}H)(Ox^{Me2})$_2$). ^{15}N NMR (THF-d_8, 71 MHz): δ -202.8 (H*N*CMe$_2$CH$_2$OC)B), -176.9 (Al(*N*CMe$_2$CH$_2$OC)$_2$B). IR (KBr, cm^{-1}): 3361 br m, 3054 s, 2981 s, 2032 s, 1580 s, 1560 s, 1462 s, 1374 s, 1296 m, 1262 m, 1204 s, 1032 m, 969 s, 734 s, 705 sh s, 679 m. Anal. Calcd for $C_{47}H_{56}B_2AlN_3O_3$: C, 74.32; H, 7.43; N, 5.53. Found: C, 73.80; H, 7.48; N, 5.10. mp 144-148 °C.

[Al(κ^2-To^M)(O^{i}Pr)$_2$] (5)

A 100 mL Schlenk flask was charged with H[To^M] (0.400 g, 1.04 mmol) and Al(O^{i}Pr)$_3$ (0.2134 g, 1.04 mmol). The solids were dissolved in 50 mL of toluene, and the solution was heated to reflux under an inert atmosphere for 24 hours. The volatile materials were removed under reduced pressure leaving the product as a tan solid (0.34 g, 0.65 mmol, 62%). ^{1}H NMR (benzene-d_6, 400 MHz): δ 7.97 (d, $^2J_{HH}$ = 7.1 Hz, 2 H, *ortho*-C$_6$H$_5$), 7.40 (vt, $^2J_{HH}$ = 7.1 Hz, 2 H, *meta*-C$_6$H$_5$), 7.22 (t, $^2J_{HH}$ = 7.1 Hz, 1 H, *para*-C$_6$H$_5$), 4.37 (septet, $^2J_{HH}$ = 5.2 Hz, 2 H, OC*H*Me$_2$), 3.68 (s, 2 H, CNCMe$_2$C*H*$_2$O), 3.45 (d, $^2J_{HH}$ = 8.5 Hz, 2 H, Al(NCMe$_2$C*H*$_2$OC)$_2$B), 3.25 (d, $^2J_{HH}$ = 8.5 Hz, 2 H, Al(NCMe$_2$C*H*$_2$OC)$_2$B), 1.37 (d, $^2J_{HH}$ = 6.2 Hz, 6 H, CH*Me*$_2$), 1.34 (d, $^2J_{HH}$ = 6.2 Hz, 6 H, CH*Me*$_2$), 1.31 (s, 6 H, CNC*Me*$_2$CH$_2$O), 1.26 (s, 6 H, CNC*Me*$_2$CH$_2$O), 1.16 (s, 6 H, CNC*Me*$_2$CH$_2$O). ^{13}C{^{1}H} NMR (benzene-d_6, 100 MHz): δ 145.3 (*ipso*-C$_6$H$_5$), 134.1 (*ortho*-C$_6$H$_5$), 127.8 (*meta*-C$_6$H$_5$), 126.1 (*para*-C$_6$H$_5$), 80.27 (Al(NCMe$_2$*C*H$_2$OC)$_2$B), 77.19 (CNCH$_2$*C*H$_2$O), 67.74 (CN*C*Me$_2$CH$_2$O), 65.7 (Al(N*C*Me$_2$CH$_2$OC)$_2$B), 64.02 (*C*HMe$_2$), 29.15 (CNC*Me*$_2$CH$_2$O) 28.33 (CH*Me*$_2$), 27.04 (Al(NC*Me*$_2$CH$_2$OC)$_2$B), 26.80 (Al(NC*Me*$_2$CH$_2$OC)$_2$B). ^{11}B NMR (benzene-d_6, 128 MHz): δ -16.6. IR (KBr, cm^{-1}): 3070 w, 3048 w, 2966 s, 2930 s, 2887 s, 2628 w, 1593 m, 1562 s sh, 1463 s, 1433 w, 1374 s, 1362 s, 1298 s, 1258 m, 1204 s, 1169 s, 1034 s br, 973 s, 850 w, 741 w, 710 s, 653 w. Anal. Calcd for $C_{27}H_{43}BAlN_3O_5$: C, 61.48; H, 8.22; N, 7.97. Found: C, 61.30; H, 8.15; N, 7.56. mp 140-145 °C.

[(κ^2-To^P)AlMe$_2$] (6)

A solution of H[To^P] (0.700 g, 1.65 mmol) in 50 mL of toluene was added to a 100 mL Schlenk flask. To this solution was added (AlMe$_3$)$_2$ (0.125 g, 1.73 mmol). Upon addition of the (AlMe$_3$)$_2$, methane production was observed as the solution bubbled vigorously for several minutes. The yellow solution was stirred for 24 hours under nitrogen. Volatiles were removed under dynamic vacuum to give the off-white product (0.503 g, 1.05 mmol, 63.6%). ^{1}H NMR (benzene-d_6, 400 MHz): δ 8.08 (d, $^2J_{HH}$ = 7.6 Hz, 2 H, *ortho*-C$_6$H$_5$), 7.44 (vt, $^2J_{HH}$ = 7.6 Hz, 2 H, *meta*-C$_6$H$_5$), 7.24 (t, $^2J_{HH}$ = 7.6 Hz, 1 H, *para*-C$_6$H$_5$), 3.95 (m, 1 H, CNCH(*i*Pr)C*H*$_2$O), 3.68 (m, 6 H, overlapping Ox^{iPr}), 3.52 (m, 1 H, Al(NCH(*i*Pr)C*H*$_2$OC)$_2$B), 3.36 (m, 1 H, Al(NCH(*i*Pr)C*H*$_2$OC)$_2$B), 2.05 (septet, $^2J_{HH}$ = 6.24 Hz, 1 H, Al(NCH(C*H*Me$_2$)CH$_2$OC)$_2$B), 1.97 (septet, $^2J_{HH}$ = 6.24 Hz, 1 H, Al(NCH(C*H*Me$_2$)CH$_2$OC)$_2$B), 1.77 (septet, $^2J_{HH}$ = 6.24 Hz, 1 H, CNCH(C*H*Me$_2$)CH$_2$O), 1.03 (d, $^2J_{HH}$ = 6.93 Hz, 3 H, Al(NCH(CH*Me*$_2$)CH$_2$OC)$_2$B), 0.93

(d, $^2J_{HH}$ = 6.93 Hz, 3 H, CNCH(CHMe_2)CH_2O), 0.84 (d, $^2J_{HH}$ = 6.93 Hz, 3 H, Al(NCH(CHMe_2)CH_2OC)$_2$B), 0.53 (d, $^2J_{HH}$ = 6.93 Hz, 3 H, Al(NCH(CHMe_2)CH_2OC)$_2$B), 0.38 (d, $^2J_{HH}$ = 6.93 Hz, 3 H, Al(NCH(CHMe_2)CH_2OC)$_2$B), 0.27 (d, $^2J_{HH}$ = 6.93 Hz, 3 H, Al(NCH(CHMe_2)CH_2OC)$_2$B), -0.29 (d, $^2J_{HH}$ = 3.47 Hz, 6 H, AlMe_2). $^{13}C\{^1H\}$ NMR (benzene-d_6, 100 MHz): δ 196.94 (br, (NCH(CHMe$_2$)CH_2OC)$_2$B), 196.04 (br, (NCH(CHMe$_2$)CH_2OC)$_2$B), 145.03 (br, *ipso*-C_6H_5), 134.35 (*ortho*-C_6H_5), 127.57 (*meta*-C_6H_5), 126.19 (*para*-C_6H_5), 73.90 (CNCH(^{i}Pr)CH_2O), 68.04 Al(NCH(^{i}Pr)CH_2OC)$_2$B), 67.97 (Al(NCH(^{i}Pr)CH_2OC)$_2$B), 67.71 (CNCH(^{i}Pr)CH_2O)$_2$B), 66.95 (Al(NCH(^{i}Pr)CH_2OC)$_2$B), 66.79 (Al(NCH(^{i}Pr)CH_2OC)$_2$B), 33.37 CNCH(CHMe$_2$)CH_2O), 30.28 (Al(NCH(CHMe$_2$)CH_2OC)$_2$B), 29.87 (Al(NCH(CHMe$_2$)CH_2OC)$_2$B), 19.05 CNCH(CHMe_2)CH_2O)), 13.92 (Al(NCH(CHMe_2)CH_2OC)$_2$B), -9.00 (AlMe), -9.30 (AlMe). ^{11}B NMR (benzene-d_6, 128 MHz): δ -16.4. IR (KBr, cm^{-1}): 3066 w, 3048 w, 2962 s, 2930 s, 2889 m, 1579 m, 1570 s, 1465 w, 1394 w, 1370 w, 1225 s, 1195 m, 990 m, 960 m, 735 w, 702 s, 680 s. Anal. Calcd for $C_{26}H_{41}BAlN_3O_3$: C, 64.89; H, 8.53; N, 8.74. Found: C, 64.40; H, 8.18; N, 8.89. mp 110-114 °C, dec.

Representative aluminum-catalyzed polymerization to give poly(lactic)acid

Rac-3,6-dimethyl-1,4-dioxane-2,5-dione (*rac*-LA) (1.64 g, 11.4 mmol) and the catalyst [(κ^2-To^M)AlMe$_2$] (0.010 g, 0.023 mmol) were loaded into a glass ampoule inside of a glovebox. The ampoule was removed, sealed under vacuum, and immersed in an oil bath at 115 °C for 24 h. The ampoule was then removed from the bath and allowed to cool to room temperature. PLA was obtained by dissolving the crude product in acetone. A portion of the crude product was used to determine the monomer conversion *via* ^{1}H NMR. The polymer was then purified by precipitation from water, and was dried under vacuum for 24 h.

DFT calculations

All calculations were performed with the NWChem software suite.[40] Density functional theory (DFT) was employed using the B3LYP hybrid functional[41] to obtain optimized geometries and frequencies (see supplementary material†). Energies were also calculated using DFT with the B3LYP functional and include the zero point energy correction. 6-311-(2d,2p) was used for aluminum and 6-311++G** basis set was used for all other atoms.[42] All structures reported have positive second derivatives with respect to coordinates, indicating that they are all minima on the potential energy surface.

Acknowledgements

At the Ames Laboratory, this research was supported by the U.S. Department of Energy, Office of Basic Energy Sciences, under Contract No. DE-AC02-07CH11358. The Department of Education is thanked for a fellowship through the GAANN program. Prof. M. Jeffries-EL is gratefully acknowledged for providing GPC analysis of poly(lactide) samples. Dr. Bruce Fulton is thanked for help with solution-state ^{15}N NMR experiments.

References

1 R. Han, A. Looney and G. Parkin, *J. Am. Chem. Soc.*, 1989, **111**, 7276–7278.
2 F.-G. Fontaine, J. Boudreau and M.-H. Thibault, *Eur. J. Inorg. Chem.*, 2008, 5439–5454.
3 (*a*) M.-H. Thibault, J. Boudreau, S. Mathiotte, F. Drouin, O. Sigouin, A. Michaud and F.-G. Fontaine, *Organometallics*, 2007, **26**, 3807–3815; (*b*) A. Fischbach, P. R. Bazinet, R. Waterman and T. D. Tilley, *Organometallics*, 2008, **27**, 1135–1139.
4 (*a*) F.-G. Fontaine and D. Zargarian, *J. Am. Chem. Soc.*, 2004, **126**, 8786–8794; (*b*) M. Sircoglou, G. Bouhadir, N. Saffon, K. Miqueu and D. Bourissou, *Organometallics*, 2008, **27**, 1675–1678.
5 M. Sircoglou, M. Mercy, N. Saffon, Y. Coppel, G. Bouhadir, L. Maron and D. Bourissou, *Angew. Chem., Int. Ed.*, 2009, **48**, 3454–3457.
6 X. Yang, C. L. Stern and T. J. Marks, *J. Am. Chem. Soc.*, 1994, **116**, 10015–10031.
7 (*a*) C. Mazet, V. Kohler and A. Pfaltz, *Angew. Chem., Int. Ed.*, 2005, **44**, 4888–4891; (*b*) V. Kohler, C. Mazet, A. Toussaint, K. Kulicke, D. Haussinger, M. Neuburger, S. Schaffner, S. Kaiser and A. Pfaltz, *Chem.–Eur. J.*, 2008, **14**, 8530–8539.
8 (*a*) C. T. Burns, D. S. Stelck, P. J. Shapiro, A. Vij, K. Kunz, G. Kehr, T. Concolino and A. L. Rheingold, *Organometallics*, 1999, **18**, 5432–5434; (*b*) P. J. Shapiro, *Eur. J. Inorg. Chem.*, 2001, 321–326.
9 S. Dagorne, S. Bellemin-Laponnaz and R. Welter, *Organometallics*, 2004, **23**, 3053–3061.
10 C. H. Dungan, W. Maringgele, A. Meller, K. Niedenzu, H. Noeth, J. Serwatowska and J. Serwatowski, *Inorg. Chem.*, 1991, **30**, 4799–4806.
11 M. H. Chisholm, N. W. Eilerts and J. C. Huffman, *Inorg. Chem.*, 1996, **35**, 445–450.
12 C. M. Dowling and G. Parkin, *Polyhedron*, 1999, **18**, 3567–3571.
13 H. V. R. Dias and W. Jin, *Inorg. Chem.*, 2003, **42**, 5034–5036.
14 A. I. Meyers and E. W. Collington, *J. Am. Chem. Soc.*, 1970, **92**, 6676–6678.
15 C. Lambert, I. Lopez-Solera and P. R. Raithby, *Organometallics*, 1996, **15**, 452–455.
16 C. M. Thomas, N. P. Mankad and J. C. Peters, *J. Am. Chem. Soc.*, 2006, **128**, 4956–4957.
17 B. Baird, A. V. Pawlikowski, J. Su, J. W. Wiench, M. Pruski and A. D. Sadow, *Inorg. Chem.*, 2008, **47**, 10208–10210.
18 J. F. Dunne, J. C. Su, A. Ellern and A. D. Sadow, *Organometallics*, 2008, **27**, 2399–2401.
19 (*a*) R. G. Kidd, in Boron-11, *NMR of newly accessible nuclei*, P. Laszlo, Academic Press, New York, 1983, Vol. 2, 49-77.; (*b*) H. Noth and B. Wrackmeyer, *NMR Basic Principles and Progress*, P. Diehl, E. Fluck, R. Kosfeld (Eds) Springer-Verlag, Berlin, 1978.
20 D. Freude and J. Haase, in *'NMR Basic Principles and Progress'*, eds P. Diehl, E. Fluck and R. Kosfeld, Springer-Verlag, Berlin, 1993, Vol. 29, p. 1.
21 L. Frydman and J. S. Harwood, *J. Am. Chem. Soc.*, 1995, **117**, 5367–5368.
22 S.-J. Hwang, C. Fernandez, J.P. Amoureux, J.-W. Han, J. Cho, S. W. Martin and M. Pruski, *J. Am. Chem. Soc.*, 1998, **120**, 7337–7346.
23 J. P. Amoureux and M. Pruski, in *'Encyclopedia of Magnetic Resonance'*, eds D. M. Grant and R. K. Harris, John Wiley & Sons, Chichester, 2002, Vol. 9, p. 226-251.
24 E. Vinogradov, P. K. Madhu and S. Vega, *Chem. Phys. Lett.*, 1999, **314**, 443–450.
25 H. Jacobsen, H. Berke, S. Doring, G. Kehr, G. Erker, R. Frohlich and O. Meyer, *Organometallics*, 1999, **18**, 1724–1735.
26 R. R. Fraser, T. S. Manour and S. J. Savard, *J. Org. Chem.*, 1995, **50**, 3232–3234.
27 (*a*) U. E. Bucher, A. Currao, R. Nesper, H. Ruegger, L. M. Venanzi and E. Younger, *Inorg. Chem.*, 1995, **34**, 66–74; (*b*) C. Foltz, D. Enders, S. Bellemin-Laponnaz, H. Wadepohl and L. H. Gade, *Chem.–Eur. J.*, 2007, **13**, 5994–6008.
28 See for example,(*a*) D. Gudat, A. Dogan, W. Kaim and A. Klein, *Magn. Reson. Chem.*, 2004, **42**, 781–787; (*b*) L. Schenetti, A. Mucci and B. Longato, *J. Chem. Soc., Dalton Trans.*, 1996, 299–303.
29 A. V. Pawlikowski, T. S. Gray, G. Schoendorff, B. Baird, A. Ellern, T. L. Windus and A. D. Sadow, *Inorg. Chim. Acta*, 2009, **362**, 4517–4525.
30 S. Trofimenko, *Acc. Chem. Res.*, 1971, **4**, 17–22.
31 J. Lewinski, J. Zachara, P. Gos, E. Grabska, T. Kopec, I. Madura, W. Marciniak and I. Prowotorow, *Chem.–Eur. J.*, 2000, **6**, 3215–3227.

32 (*a*) D. White, B. C. Taverner, P. G. L. Leach and N. J. Coville, *J. Comput. Chem.*, 1993, **14**, 1042–1049; (*b*) D. White and N. J. Coville, *Adv. Organomet. Chem.*, 1994, **36**, 95–158; (*c*) I. A. Guzei and M. Wendt M., *Dalton Trans.*, 2006, 3991–3999.
33 I. A. Guzei, M. Wendt, *Program Solid-G*. UW-Madison, WI, USA, 2004.
34 (*a*) R. G. Ball, C. K. Ghosh, J. K. Hoyano, A. D. McMaster and W. A. G. Graham, *J. Chem. Soc., Chem. Commun.*, 1989, 341–342; (*b*) M. Bovens, T. Gerfin, V. Gramlich, W. Petter, L. M. Venanzi, M. T. Haward, S. A. Jackson and O. Eisenstein, *New J. Chem.*, 1992, **16**, 337–345; (*c*) R. E. Cowley, R. P. Bontchev, E. N. Duesler and J. M. Smith, *Inorg. Chem.*, 2006, **45**, 9771–9779.
35 R. D. Shannon, *Acta Crystallogr., Sect. A: Cryst. Phys., Diffr., Theor. Gen. Crystallogr.*, 1976, **32**, 751–767.
36 O. Dechy-Cabaret, B. Martin-Vaca and D. Bourissou, *Chem. Rev.*, 2004, **104**, 6147–6176.
37 For recent examples of aluminum-catalyzed lactide polymerization, see: (*a*) Z. Zhong, P. J. Dijkstra and J. Feijen, *Angew. Chem., Int. Ed.*, 2002, **41**, 4510–4513; (*b*) Z. Tang, Y. Yang, X. Pang, J. Hu, X. Chen, N. Hu and X. Jing, *J. Appl. Polym. Sci.*, 2005, **98**, 102–108; (*c*) N. Nomura, R. Ishii, Y. Yamamoto and T. Kondo, *Chem.–Eur. J.*, 2007, **13**, 4433–4451; (*d*) M. Bouyahyi, E. Grunova, N. Marquet, E. Kirillov, C. M. Thomas, T. Roisnel and J.-F. Carpentier, *Organometallics*, 2008, **27**, 5815–5825; (*e*) A. Alaaeddine, C. M. Thomas, T. Roisnel and J.-F. Carpentier, *Organometallics*, 2009, **28**, 1469–1475.
38 H. Li, C. Wang, F. Bai, J. Yue and H.-G. Woo, *Organometallics*, 2004, **23**, 1411–1415.
39 (*a*) J. E. Kasperczyk, *Macromolecules*, 1995, **28**, 3937–3939; (*b*) K. A. M. Thakur, R. T. Kean, E. S. Hall, J. J. Kolstad, T. A. Lindgren, M. A. Doscotch, J. I. Siepmann and E. J. Munson, *Macromolecules*, 1997, **30**, 2422–2428.
40 (*a*) R. A. Kendall, E. Apra, D. E. Bernholdt, E. J. Bylaska, M. Dupuis, G. I. Fann, R. J. Harrison, J. Ju, J. A. Nichols, J. Nieplocha, T. P. Straatsma, T. L. Windus and A. T. Wong, *Computer Phys. Comm.*, 2000, **128**, 260–283; (*b*) E. J. Bylaska, W. A. d. Jong, N. Govind, K. Kowalski, T. P. Straatsma, M. Valiev, D. Wang, E. Apra, T. L. Windus, J. Hammond, P. Nichols, S. Hirata, M. T. Hackler, Y. Zhao, P.-D. Fan, R. J. Harrison, M. Dupuis, D. M. A. Smith, J. Nieplocha, V. Tipparaju, M. Krishnan, Q. Wu, T. V. Voorhis, A. A. Auer, M. Nooijen, E. Brown, G. Cisneros, G. I. Fann, H. Fruchtl, J. Garza, K. Hirao, R. Kendall, J. A. Nichols, K. Tsemekhman, K. Wolinski, J. Anchell, D. Bernholdt, P. Borowski, T. Clark, D. Clerc, H. Dachsel, M. Deegan, K. Dyall, D. Elwood, E. Glendening, M. Gutowski, A. Hess, J. Jaffe, B. Johnson, J. Ju, R. Kobayashi, R. Kutteh, Z. Lin, R. Littlefield, X. Long, B. Meng, T. Nakajima, S. Niu, L. Pollack, M. Rosing, G. Sandrone, M. Stave, H. Taylor, G. Thomas, J. v. Lenthe, A. Wong, Z. Zhang, Pacific Northwest National Laboratory Richland, Washington 99352, USA, 2007.
41 (*a*) A. D. Becke, *J. Chem. Phys.*, 1993, **98**, 5648–5652; (*b*) C. T. Lee, W. T. Yang and R. G. Parr, *Phys. Rev. B*, 1988, **37**, 785–789.
42 M. J. Frisch, J. A. Pople and J. S. Binkley, *J. Chem. Phys.*, 1984, **80**, 3265–3269.